Hermann Hausen[1] and Wolfgang Schüle[1]

IRRADIATION CREEP IN NICKEL CONTAINING AND IN MANGANESE CONTAINING STAINLESS STEEL ALLOYS

REFERENCE: Hausen, H. and Schüle, W., **"Irradiation Creep in Nickel Containing and in Manganese Containing Stainless Steel Alloys,"** *Effects of Radiation on Materials: 18th International Symposium, ASTM STP 1325,* R. K. Nanstad, M. L. Hamilton, F. A. Garner, and A. S. Kumar, Eds., American Society for Testing and Materials, 1999.

ABSTRACT: This is a final report on the results of measurements of neutron irradiation creep which have been performed in non-instrumented creep rigs (Trieste) on many different stainless steel alloys during the last fifteen years in high flux positions in the High Flux Reactor (HFR) at Petten. The creep elongations were measured in hot cells during reactor shut down periods. A few investigations of the creep elongation were performed in fully instrumented creep rigs (Crisp).

All the materials were irradiated in the as-received state, which was usually a type of solution-annealed state, after annealing at 400, or at 600, or at 800°C, and after 20% cold work. The irradiation temperature ranged from 300 to 500°C and the applied stresses were between 25 and 300 MPa.

The variations in length found up to irradiation doses of about 5 dpa are mainly attributed to the formation of radiation-induced microstructural changes, which are connected either with increases or with decreases in the volume of the materials. We are advancing an interpretation of the data which is not without contradictions. We believe that among the many microstructural changes only the formation of carbides, which is connected with an increase in volume, and only the formation of α-ferrite, which is connected with a decrease in volume, are of importance. The α-ferrite phase is very brittle, decreasing the ductility of the stainless steels dramatically.

An almost thermal equilibrium state of microstructure while irradiating with high energy particles is obtained after about 5 dpa, depending also on the irradiation temperature. The increase in length obtained for doses larger than 5 dpa is attributed mainly to irradiation creep. The normalized creep rates for all stainless steel materials are almost equal in HFR, ORR, and in EBR II. The creep rates increase linearly with stress and flux, and they are slightly dependent on the irradiation temperature ($Q_{irr.}$= 0.132 eV) for irradiation temperatures below about 450°C. For irradiation temperatures above 450°C a contribution of thermal vacancies to irradiation creep is noticed and the irradiation creep rates can no longer be ascribed to a simple irradiation creep relation.

KEYWORDS: neutron irradiation creep, High Flux Reactor at Petten, Oak Ridge Research Reactor, and Experimental Breeder Reactor II at Idaho, stainless steel alloys, microstructure, α-ferrite, carbides, radiation damage, phase diagram

[1] Institut für Angewandte Physik der Johann Wolfgang Goethe-Universität Frankfurt, Robert Mayer Straße 2-4, D-60054 Frankfurt, Germany.
Present address: Via Bosco 23, I-21038 Leggiuno (Va), Italy.

Copyright© 1999 by ASTM International www.astm.org

Investigations of irradiation creep on various types of stainless steel alloys have been performed for many years in many different laboratories all over the world. The main important results obtained are reported in the many Proceedings of the International Symposia on Effects of Radiation on the Microstructure of Materials [1]. One of the important results is seen in the finding that in general irradiation creep is relatively small but substantially larger than that produced by thermal creep. However, this finding is not sufficient to recommend stainless steel alloys for nuclear reactor devices, apart from the fact that the acceptable creep elongation in a fusion device is still not defined, because the microstructures formed during irradiation in stainless steel alloys may be brittle structures. A recent review on results of investigations of irradiation creep is given by F. A. Garner [2]. He also considers the many phases which are found in stainless steel alloys with and without high energy particle irradiation and the volume changes connected with these phases.

There are numerous and sometimes contradictory phase diagrams of nickel-containing stainless steel alloys in the literature also taking into account the various additions such as C, Ti, Mo, Mn, Nb, Cu, Al, Si, N, S, etc. as single additions or in a combination of many additions. There are a very few metallurgists who know the purpose of and the reason for each addition, and only very few of the additions may be of importance in an irradiation environment. However, the many additions in the very few types of stainless steel alloys, which were tested in the past for their radiation resistance, made it almost impossible to interpret and to understand the results. A few phases and compounds are listed to give the reader an idea on the complexity of the problem: Laves-, α-ferrite-, α'-martensite-, γ-austenite-, γ'-, γ''-, δ-, β-, σ-, χ-, μ-, G-, R-phase (This list consists of almost all the letters in the Greek alphabet.), and compounds such as carbides, nitrides, sulfides etc.. Most of these phases (and compounds) become dissolved during a solution anneal at 1100°C, but these phases are again formed during quenching, cooling, or aging after a solution anneal. The formation of all these phases is usually associated with volume changes, and for this reason it is better to use well aged stainless steel alloys in an irradiation environment and not a material in the as-received state which is meant to be the solution-annealed state.

If a stainless steel material is irradiated with high energy particles then the composition of all these mentioned phases will change, e. g. most of these mentioned phases become enriched in Ni with respect to Fe and Cr by radiation-enhanced diffusion, because nickel is the faster diffusing element when it diffuses via an interstitialcy diffusion mechanism. This will result in a depletion of nickel in the austenitic γ-phase. Further, new phases (unknown?) will be formed by radiation-enhanced diffusion, which are not formed without radiation, because the atoms are insufficiently mobile at relevant low temperatures.

Below a characteristic temperature, which is about 340°C in stainless steel alloys, radiation-induced structures, e.g. agglomerates of interstitials, are formed, which grow and lead to a dynamic equilibrium concentration of dislocations. If the stainless steel alloys contain under-sized atoms, e.g. Si, then the agglomerates of interstitials are enriched in silicon and radiation-induced Ni-Si-precipitates are formed. This means that the γ-phase becomes further diluted in nickel.

We have previously shown that perhaps only two phases formed during irradiation are of importance, especially for irradiation creep and that all the other mentioned phases formed may cause negligibly small property changes. We found that the formation of carbides causes an increase in volume, i.e. an increase in the elongation during irradiation

[3], and that the formation of α-ferrite causes a decrease in the volume, i.e. a decrease in the elongation. In the present work we will give further arguments for this interpretation knowing that we are in some instances in difficulty with our interpretation.

We believe that we found that nucleation sites are necessary for the formation of α-ferrite. Dislocations, or α'-martensite, or stress application, or just irradiation with high energy particles can cause nucleation. The α-ferrite phase is thus formed via radiation-enhanced diffusion. M. Grossbeck et al. found that 316L stainless steel alloys became so brittle on irradiating them at 60°C after very small irradiation doses that they broke before the first elongation test could be performed [4]. We report at this conference a similar finding on irradiating at 100°C [5]. The question is, whether the amount of α-ferrite formed at low irradiation temperatures is sufficient that the samples break or whether the α-ferrite formed during irradiation transforms at low temperatures, i.e. below its brittle-ductile transition temperature, into the very brittle α'-martensite.

D. R. Harries suggested that the α-ferrite we claim to have obtained would be α'-martensite[2]. We do not want to reject this interpretation, because our interpretation does not stand on too safe grounds, but we will mention a few arguments, which we believe, are in favour of our interpretation. We found that α-ferrite is already formed at "high" irradiation temperatures, e.g. at 400°C, and that it is not formed spontaneously. The temperature of 400°C is well above the martensitic transition temperature. It is further found that the amount of formation of α-ferrite decreases drastically with decreasing irradiation temperature. This finding is not in contradiction to either interpretation because diffusion is necessary for the formation of the α-ferrite-phase as well as for the formation of α'-martensite. In the latter case the depletion of nickel from the austenitic γ-phase causes an increase of the martensitic transition temperature so that finally α'-martensite is formed sponaneously at the irradiation temperature.

When this investigation was started many years ago the phase diagram of maganese-containing stainless steel alloys was not known below about 600°C. It was thought that the γ -phase field would be as extended in the nickel-containing stainless steel alloys. We worked for some years on the manganese-containing stainless steel alloy phase diagram [6] and we found that the γ-phase field is very narrow and almost disappears below 400°C in these alloys. The α-Mn phase is the phase adjacent to the γ-phase in direction to the chromium corner. The α-Mn phase is ductile if it does not contain chromium and it is very brittle if it contains about 20% Cr. This phase always forms readily and almost no incubation time was observed for its formation. The α-ferrite phase is not only a very brittle phase in the manganese-containing stainless steel alloys, but the volume change connected with its formation is large so that samples change their shape during annealing when this phase is formed. We did not find the many phases which were observed in nickel-containing stainless steel alloys and which were mentioned in this work, because for the studies on the phase diagram, almost "pure" stainless steel alloys were used. We also believe that many phases are also present in the AMCR-type alloys, because these alloys contain many different elements as additions similar to those put into the 316L-type alloys.

There is a peculiarity between the nickel and the manganese containing stainless steel alloys, because in the latter alloys a reversible hexagonal martenistic ε-phase showing no

2 D. R. Harries, private communication.

hystersis is formed below about 200°C[3]. The formation of this phase is connected with a volume change. Therefore, the creep data obtained after irradiation in the Trieste-rigs at ambient temperature in hot cells were compared with irradiation creep data obtained in-situ during irradiation in a Crisp-rig which is a fully instrumented creep rig.

The 316L and the AMCR stainless steel alloys remain fully austenitic during cooling from 1000°C to ambient temperature, and also during a subsequent heating between ambient temperature and 1000°C [6]. These observations lead to the opinion that these materials are single phase materials in the entire temperature range of interest and that this feature is also maintained on irradiating them at any temperature. However, if AMCR-type material is plastically deformed at ambient temperature α-ferrite is formed readily during annealing above the temperature, above which the component atoms in stainless steel alloys are sufficiently mobile, i.e. above 300°C. In 316L alloys α-ferrite is only formed during annealing if the cold-work is performed prior to annealing at temperatures well below ambient temperature.

In order to obtain more information on the processes occuring during irradiation we irradiated "pure" manganese-containing stainless steel materials, varying the composition of the main components, namely of iron, chromium and nickel, and also the amount of carbon, titanium, and silicon. In part we failed to complete this research because the titanium containing alloys were very brittle due to the formation of titanium carbides so that it was impossible to deform them plastically at high temperatures, e.g. at 300°C. However, in some of these materials we were able to study the formation of carbides and also of α-ferrite during irradiation under an applied stress.

One of us (W. Sch.) many years ago suggested that the European Union should determine the microstructures formed during irradiation at various temperatures for various doses on materials differently treated prior to irradiation. However, no money has so far been allocated to this research and about three hundred specimens are still in storage and available for future examinations.

In the following we will present the main results obtained in the last fifteen years on irradiating 343 specimens in the High Flux Reactor (HFR) at Petten, The Netherlands. The results will be compared with similar results obtained in ORR at Oak Ridge and in EBR II at Idaho.

EXPERIMENTS

Materials

The compositions of the stainless steel materials used in the present investigation are listed in Table I. The American stainless steel materials, namely US PCA and US 316, were obtained from the Metals and Ceramics Division of the Oak Ridge National Laboratory in 20% cold-worked bars in connection with the Implementing Agreement, which was drawn up by the International Atomic Energy Agency in Vienna many years ago and through which various stainless steel materials were exchanged between various countries, namely Japan,

[3] The existence of an ε-phase is also reported for nickel-containing stainless steel alloys, the transition temperature of which is found below ambient temperature.

the USA, the European countries, and the states of the former Soviet Union, to be tested in the high flux reactors of the respective countries. The European reference steel 316L, and AMCR 0033, AMCR 0034, and AMCR 0035 were obtained from Creusot-Loire (France) in the solution annealed state in large plates having a cross section of 15 cm x 3 cm and a length of about 300 cm. The AMCR 7758, AMCR 7761, and AMCR 7763 materials were obtained from Vakuum Schmelze, Hanau, Germany, in the solution-annealed state in rods having a diameter of 1.0 cm and a length of 500 cm. The final dimensions of the rods were obtained by hot-rolling. However, the preparation of these alloy materials was very difficult because most of the alloy materials, which were all prepared by hot-rolling, contained many cracks and only the three alloys listed here and subsequently investigated were obtained without cracks.

Table I
The composition of stainless steel alloys in weight percent investigated in the present work

Steel	C	Mn	Ni	Cr	Si	Mo	Ti	N	S	P
US PCA	0.06	1.5 - 2.3	15 - 17	13 - 15	0.4 - 0.6	1.8 - 2.2	0.2 - 0.4	-	-	-
US 316	0.06	2.0	10 - 14	16 - 18	1.0	2.3	0.2 - 0.3	-	-	-
Eur.Ref.	0.024	1.81	12.32	17.44	0.46	2.5	-	0.06	0.002	0.027
AMCR 0033	0.105	17.50	< 0.10	10.12	0.555	< 0.06	-	0.19	0.008	0.016
AMCR 0034	0.100	17.69	0.15	10.11	0.64	1.52	-	0.16	0.008	0.025
AMCR 0035	0.029	19.88	0.265	14.09	0.63	< 0.06	-	0.048	0.006	0.018
AMCR 7758	0.062	28.6	-	10.0	0.87	-	0.87	-	-	-
AMCR 7761	0.11	29.4	-	10.2	1.01	-	-	-	-	-
AMCR 7763	0.10	19.4	-	10.2	0.94	-	0.85	-	-	-

Bars were cut from the plate materials. They had a cross section of 1.5 cm x 1.5 cm and a length of 10 cm. Some of these bars were 10 or 20% cold-worked in the direction of the length of the bars and then these bars were machined to samples having a length of 5.6 cm with measuring shoulders 5.0 cm apart. In the Trieste-rig seven specimens were always clamped together in one stem, one specimen behind the other. Thus 49 specimens were irradiated in seven stems in one Trieste-rig. The stress applied to a specimen was obtained from the load applied to the stem and the diameter of the specimen, which was varied accordingly between 1.5 and 3 mm. The samples were machined by means of two motors working synchronously on the beginning and on the end of the specimen. After the machining some of the materials were annealed at 400, or 600, or 800°C for 1 h in an inert gas atmosphere or in a vacuum better than 10^{-5} torr[4].

[4] At the beginning of this research, fifteen years ago, the intention was to use solution annealed-steals for the first wall of a fusion reactor. However, the solution-annealed state which is a state in thermal equilibrium at 1050°C can not be maintained in pieces as large as those used as starting materials in the present work. This equilibrium state can also not be maintained in the large pieces from which the parts will be fabricated for a fusion reactor. Since almost all micro-structural changes are connected with volume changes in a material aging the materials prior to machining is recommended.

The samples obtained from AMCR 7758, AMCR 7761, and AMCR 7763 rod materials were prepared in the same way as those prepared from plate materials, except that no rod materials were cold-worked prior to irradiation.

The samples for the Crisp facility were prepared in the same way as the samples for the Trieste facility. The total length of the samples was 14.7 cm, the measuring length was 10.0 cm and the measuring shoulders were 11.5 cm apart.

Trieste Irradiation Facility

The entire high temperature experimental Trieste programme comprises seven irradiation facilities in which samples were irradiated at temperatures between about 300 and 500°C. In one Trieste irradiation facility, a total of 49 tensile samples and a large number of reference half-shell pairs are irradiated under various combinations of temperature and stress. A single sample column, which is also called a stem, comprises seven cylindrical dumbbell-shaped tensile samples associated with reference shells, all contained in a supporting tube. Seven independent sample columns are inserted into separate channels of the Trieste carrier. The columns can be loaded independently by a self-contained spring washer system at the head of the stems.

The stresses in the tensile samples were set to 25, 50, 75, 100, 150, 200, 250, and 300 MPa. The corresponding tensile loads on the sample columns are adjusted to an accuracy of ± 2%. However, the scatter of the measuring data was sometimes much larger than 2%. We believe that the martensitic ε-phase, which is formed in manganese containing stainless steel alloys below about 200°C and the formation of which is connected with a volume change, was not always complete.

The strain measurements on the individual tensile samples were performed out of pile in hot cells through slot-shaped windows in the supporting tubes by a photo-electric incremental linear measuring system. Dimensional changes of ± 1.5 μm can be detected, which in turn corresponds to a measuring accuracy of about ± 2%.

The irradiation temperatures were obtained by controlling gas mixtures in a stepped gap between the specimen carrier and the outer reloadable thimble. In a high flux channel of the HFR at Petten irradiation temperatures between 300 and 620°C can be obtained. In the present experiments no temperature control was provided during irradiation. Prior to irradiation the irradiation temperatures were determined in a dummy Trieste rig by means of thermo-couples. Thus a variation of the irradiation temperature of ± 10°C must be taken into account.

The irradiations were performed in the G-type high flux channels. Neutron metrology was performed by evaluating activation detectors which are installed inside each of the unstressed reference half-shells. The fluence values are determined with an accuracy of ± 10% for each of the G-channels. The neutron flux in channel G3/G7 in the HFR at Petten was $\phi = 2 \cdot 10^{14}$ n·cm^{-2} (E>0.1 MeV n) which corresponds to a displacement rate of K= $1.7 \cdot 10^{-7}$ dpa·s^{-1} according to the Hip-Teddi code [7].

Crisp Irradiation Facility

In the Crisp device the irradiation creep elongation of three samples in three different rigs can be measured simultaneously. All three rigs, combined in one irradiation facility, are independent with respect to the irradiation temperature and the applied stresses which can be varied between 300 and 600°C, and between 25 and 300 MPa, respectively. The experimental program comprises three irradiation thimbles with a total of nine individual creep rigs.

In each rig a single dumbbell-shaped sample, which is submerged in NaK, is stressed in tension by a bellows system. The stresses were adjusted with an accuracy of ± 2%. Strain measurements are taken semicontinuously by comparing the sample length with the length of an unstressed reference piece of the same material. Length changes are detected by a remotely controlled displacement transducer. Dimensional changes can be detected with a precision of ± 2.5 %. In order to measure thermal creep strains the irradiation temperatures were maintained during reactor shut-down periods by built-in electrical heaters.

RESULTS AND DISCUSSION

Materials Irradiated in the Trieste Rig

The AMCR 0033 alloy is of all the alloys listed in Table I the alloy most extensively investigated in the present work. The most important results obtained for this alloy are presented and a few charateristic results for the other alloys are presented as well.

The AMCR 0033 materials were obtained in huge bars in the solution annealed state. However, huge bars can not cool sufficiently fast that the solution annealed state is maintained. In order to irradiate a rather well defined state we not only irradiated materials in the "as-received state" (A), but we also annealed the materials for some hours at e. g. 400 and 600°C, respectively, prior to irradiation.

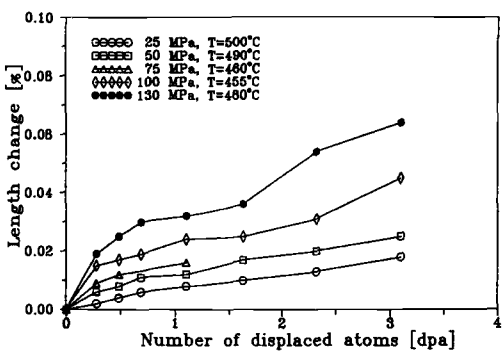

Fig. 1.
The changes in the length of five samples of solution annealed AMCR 0033 are plotted versus the number of displaced atoms. The irradiation temperatures and the respective applied stresses are listed in the figure. The samples were annealed for one hour at 400°C prior to irradiation.

The length changes for various applied stresses and for approximately one irradiation temperature (455-500°C) are plotted versus the number of displaced atoms, i.e. the irradiation dose, in Fig. 1. It is noticed that the length changes for a certain number of displaced atoms increases with increasing applied stress. The shape of the curves are similar to those obtained in a thermal creep experiment, where one distinguishes between a primary and a secondary creep stage. However, this nomenclature has almost nothing to do with the present finding. We have shown previously [3] and we will show again in this work, that the observed length changes in Fig. 1 are mainly due to volume changes connected with microstructural changes caused by diffusion of radiation-induced point defects and not to irradiation creep itself. The observed changes in length are consequently a result of a superposition of two processes, namely of the formation of carbides, the formation of which is connected with an increase in volume, and the formation of α-ferrite, the formation of which is connected with a decrease in volume. The rate of formation of each process depends on the irradiation temperature and is different for both processes. In the following we call the length changes caused by the formation of microstructure during irradiation the "primary creep stage" and the length change at the beginning of an irradiation "primary creep stage I" and the subsequent change in length "primary creep stage II" (Fig. 1). The rate of the change in length in the primary creep stage II shown in the present figure is approximately the irradiation creep rate of the "secondary creep stage", which is approximately obtained for irradiation doses larger than about 5 dpa, depending also on the irradiation temperature, and which is considered to be mainly due to irradiation creep.

The variation in length of 20% cold-worked AMCR 0033 material is plotted versus the number of displaced atoms for various applied stresses in Fig. 2. The irradiation temperature was between 320 and 350°C.

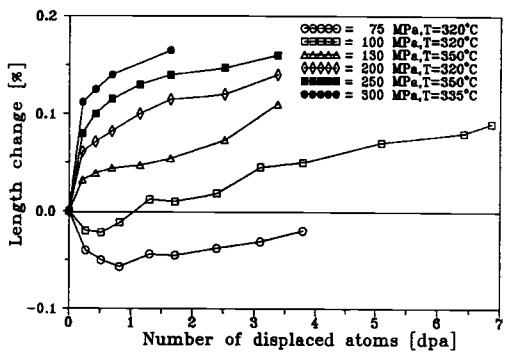

Fig. 2.
The changes in the length of six samples of AMCR 0033 are plotted versus the number of displaced atoms. The irradiation temperatures and the respective applied stresses are listed in the figure. The samples were 20 % cold-worked prior to irradiation.

It is evident that the amount of increase in length in primary creep stage I decreases with decreasing applied stress and even a decrease in length is observed at the beginning of the irradiation for 100 and 75 MPa. This latter observation confirms our previous conclusion concerning the superposition of the effect of two microstructural processes, which causes an increase and a decrease in volume, respectively. In addition, the volume change, i.e. the

amount of the decrease in length in primary creep stage I, increases drastically with decreasing applied stress. We conclude that the amount of α-ferrite formed increases drastically with decreasing applied stress and that no increase in volume due to the formation of carbides is noticed any longer. We are here in a situation, where we must explain the difference in the findings shown in Figs. 1 and 2.

For the formation of α-ferrite, nucleation sites are necessary and apparently 20% cold-work increased the number of nucleation sites in comparison to the number of nucleation sites present in annealed material and formed during irradiation (Fig. 2), so that the amount of α-ferrite formed is much larger in cold-worked material than in the annealed material. Further, the amount of α-ferrite formed increases with decreasing applied stress. The rate of the variation in length in primary creep stage II is for all stresses about equal within the error limits and different from the creep rates in the secondary creep stage, which is not shown in Fig. 2. The phenomenon of the secondary creep rate, which is obtained for doses larger than 5 dpa, will be discussed in a later section of this work.

In Fig. 3 we plotted the length changes of 20% cold-worked AMCR 0033 for an applied stress of 75-130 MPa versus the number of displaced atoms. The irradiation temperatures decreased from 480 to 320°C, and the amount, by which the length of the samples decreases, decreases with decreasing irradiation temperature. We conclude that the amount of α-ferrite formed increases with decreasing irradiation temperature.

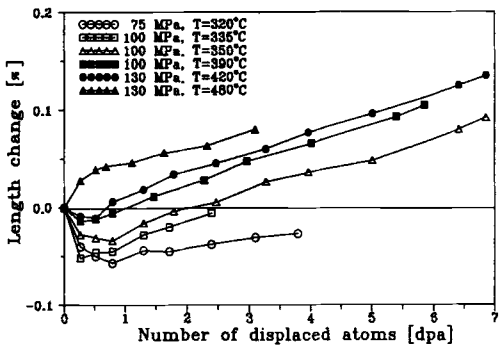

Fig. 3.
The changes in the length of samples of AMCR 0033 are plotted versus the number of displaced atoms. The irradiation temperatures, and the respective applied stresses are listed in the figure. The samples were 20% cold-worked prior to irradiation.

These features, namely that the amount of α-ferrite formed during irradiation increases with decreasing applied stress for a constant irradiation temperature and with decreasing irradiation temperature for a constant applied stress (Figs. 2 and 3) suggest that this phase is formed by radiation-induced point defects and not spontaneously as α'-martensite.

We already have mentioned that the AMCR 0033 alloy remains austenite, if it is slowly cooled from 1000°C to ambient temperature and subsequently again slowly heated to 1000°C. However, if this material is cold-worked prior to heating, α-ferrite is formed during heating above 300°C and dissolved during further heating at about 600°C [6]. This means that nucleation sites are necessary for the formation of this phase. If AMCR 0033 is irradiated in the as-received state or in an annealed state (Fig. 1) a small decrease in the

length is observed at the beginning of the irradiation for small applied stresses and low irradiation temperatures. We assume that irradiation with high energy particles also provides nucleation sites so that α-ferrite is formed, but that the number of nucleation sites provided by the irradiation is much smaller than that obtained by a cold-work, and that consequently the rate of α-ferrite formed in annealed AMCR 0033 during irradiation is much smaller than in a cold-worked material, for equal irradiation doses.

If cold-worked AMCR 0033 is annealed at about 350°C α-ferrite is formed in a very sluggish way within a few days. If the annealing is continued at 350°C then after an annealing time of about six weeks all the α-ferrite formed previously is completely dissolved[5]. This means that α-ferrite is formed if nucleation sites are provided but that this phase is not a thermal equilibrium phase for AMCR 0033 at 350°C. However, this phase was found after irradiation [8] and we believe that α-ferrite becomes a quasi-thermal equilibrium phase when irradiating below about 600°C, because irradiation provides continuously nucleation sites.

If AMCR is cold-worked prior to heating at 600°C the original form of the specimen is drastically changed, indicating that the formation and dissolution of α-ferrite is connected with large volume changes of the material, and in addition many cracks are found[5]. Thus the α-ferrite phase in AMCR 0033 is a very brittle phase.

The variation in length of 20% cold-worked US 316 steels (Table I) during irradiation in the HFR at Petten is shown in Fig. 4.

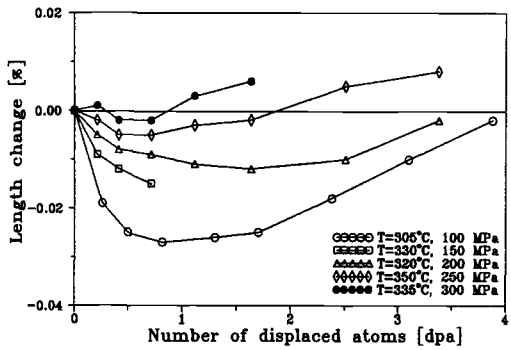

Fig. 4.
The changes in the length of five samples of US 316 are plotted versus the number of displaced atoms. The irradiation temperatures, and the respective applied stresses are listed in the figure. The samples were 20% cold-worked prior to irradiation.

In this material a decrease in the elongation is found at the beginning of the irradiation, the amount of which increases with decreasing applied stress. We believe that this phenomenon, namely the decrease in elongation in primary creep stage I, can be explained by assuming that α-ferrite is also formed in US 316 in a similar way as in AMCR 0033.

Alloy 316L is in many respects different from alloy AMCR 0033, e.g. the α-ferrite phase is not formed during annealing after a cold-work at ambient temperature. However, if

5 W. Schüle, to be published

the cold-work is performed below ambient temperature this phase also develops during subsequent annealing. We found in the present work (Figs. 3 and 4) that the variations in length with irradiation time, irradiation temperature and applied stress are very similar for both alloys (Figs. 3 and 4). We conclude from this feature that the decrease in length in the US 316 steels is also due to the formation of α-ferrite during irradiation. The α-ferrite formed in the 316 type steels must also be a very brittle phase because even low dose irradiations at 60°C and at 100°C cause fracture [4,5].

We also irradiated 20% cold-worked US 316 steels after an anneal of one hour at 700°C. Previously we found that after an anneal of 30 min. at 700°C the recovery of work-hardening was almost completed, i.e. dislocations introduced by cold-work were annealed. The irradiation temperature for the various specimens was varied between 455 and 500°C and the applied stresses between 25 and 130 MPa. A small decrease in length was only observed for 25 and 50 MPa and an increase in length for 75, 100, and 130 MPa. The increase in length for 130 MPa was very large after about one dpa namely 0.16%. We believe that the yield stress of annealed US 316 is also of the order of 130 MPa, and that the material was slightly plsatically deformed during irradiation for an applied stress of 130 MPa.

We found small decreases in length in primary creep stage I in annealed AMCR 0034 and AMCR 0035, in AMCR 7758, in US 316, and in European reference steels. We did not find a decrease in length in annealed alloys of type AMCR 0033, AMCR 7761, AMCR 7763, and US PCA. All together the irradiation temperatures and the applied stresses for the latter materials were not in favour of the detection of decreases in length. But, in general the changes in length were similar to those reported for AMCR 0033 in Fig. 1 and we interpret this accordingly, namely that the observed variations in length are due to a superposition of two processes: the formation of carbides causes an increase in the length and the formation of α-ferrite causes a decrease in length. We also believe that the amount of α-ferrite formed during irradiation increases with decreasing applied stress and with decreasing irradiation temperature. We will show later in this work that e.g. the increase in volume due to the formation of titanium carbide in e.g. AMCR 7763 is much larger than the decrease in volume due to the formation of α-ferrite, so that in total only a large increase in length is obtained during irradiation.

In the following we shall discuss results which were obtained on various types of stainless steel alloys; results which fit the scheme of experimental results presented so far and which are seemingly in contrast to this scheme, and we shall also try to explain these latter data.

The length changes of three samples are plotted versus the number of displaced atoms in Fig. 5. If we assume that the variations in length are due to volume changes and if we follow our previous nomenclature then primary creep stage I ends for the sample, which was irradiated in the as-received state at 0.3 or 0.9 dpa, and for the two other samples, which were annealed prior to irradiation, at 0.3 dpa, and primary creep stage II begins after these irradiation doses, respectively. Primary creep stage II ends at about 5 dpa and is about equal to the creep rate of the secondary creep stage.

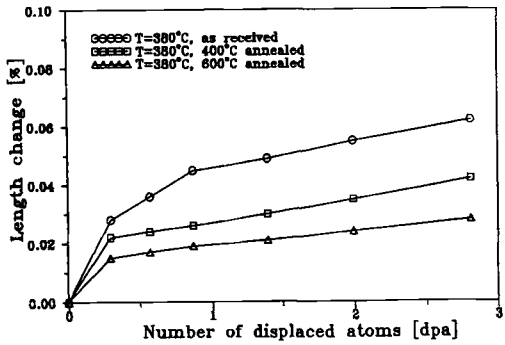

Fig. 5
The length changes of three samples of AMCR 0033 are plotted versus the number of displaced atoms. The irradiation temperature was $T_{irr.}$ = 380°C for all three specimens, and the stress was 50 MPa. The samples were irradiated in the as-received state (A), and in the annealed state at 400 and 600°C, respectively.

The length change for the specimen irradiated in the as-received state is larger than that found after an anneal at 400°C and is in turn larger than that found after an anneal at 600°C. This feature was observed frequently and has already been reported [2,9]. It is less pronounced for 25 MPa and more pronounced for 100 MPa. We believe that the specimen in the as-received state, which was slowly cooled from the solution-annealed state, contains a smaller number of carbides than the specimens annealed prior to irradiation for one hour at 400 and 600°C, respectively. Thus the amount of increase in length in primary creep stage I reflects the formation of carbides during irradiation, which is more marked in the samples in which the amount of carbides prior to irradiation is smaller.

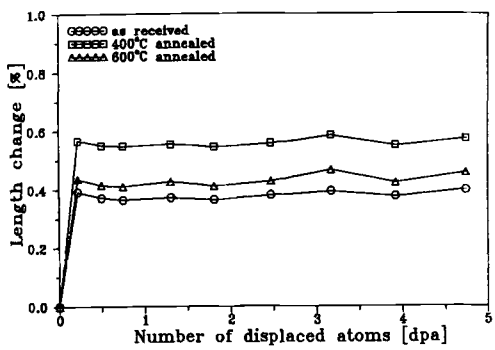

Fig. 6.
The changes in the length of three samples of AMCR 0033 are plotted versus the number of displaced atoms. The irradiation temperature was $T_{irr.}$ = 370°C, and the applied stress was 200 MPa. The samples were irradiated in the as-received state (A), and in the annealed state at 400 and 600°C, respectively.

Similar observations which have been reported in Fig. 5 for AMCR 0033 were also obtained for AMCR 0034 and AMCR 0035. However, the sequence obtained for AMCR 0033, namely that the materials in the as-received state show the largest length change during irradiation followed by the samples annealed at 400 and 600°C, is broken for the two other AMCR alloys, e.g. the materials in the as-received state showed the smallest length change with respect to the materials annealed prior to irradiation.. We believe that the as-received state was different in these two materials from that in AMCR 0033, that e.g. more

carbides are formed during cooling from the solution annealed state in these two materials than in AMCR 0033.

When a stress of 200 MPa is applied, which is almost twice the yield stress of annealed AMCR 0033, a length change of about 0.5% is found at the beginning of the irradiation (Fig. 6). Thus, the increase in length does not correspond to primary creep stage I and is attributed mainly to a change in length due to plastic deformation occuring for an applied stress of 200 MPa, i.e. due to work-hardening. The primary creep stage I and II begins after an irradiation dose of 0.2 dpa and is almost zero. Thus an almost complete compensation of the volume changes due to the formation of carbides and of α-ferrite is obtained, and we do not know at which irradiation dose the secondary creep stage starts.

In Fig. 7 we plotted length changes of samples of untreated AMCR 0033 (in the as-received state (A)) prior to irradiation as a function of the irradiation dose for 25, 50, 100, and 130 MPa. It is recognized that the length changes obtained in primary creep stage II is almost independent of the irradiation dose, similar to those reported in Fig. 6, and that the total elongation obtained decreases with increasing applied stress. The irradiation temperatures of the samples varied between 350 and 400°C, and the damage rate between $\Phi = 3.2 \cdot 10^{-5}$ to $\Phi = 1.4 \cdot 10^{-4}$ dpa·s^{-1}. A very similar observation was made only once before for a material which was annealed for one hour at 600°C prior to irradiation.

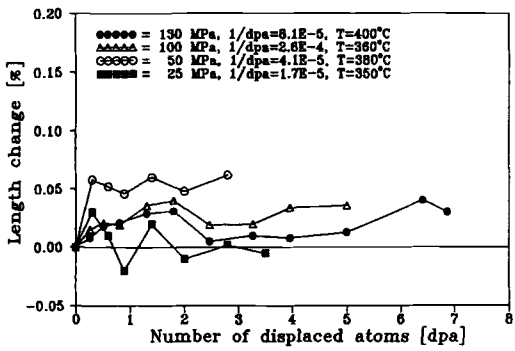

Fig. 7.
The changes in the length of four samples of AMCR 0033 are plotted versus the number of displaced atoms. The irradiation temperature and the respective applied stresses together with the damage rates are listed in the figure. The samples were irradiated in the as-received state.

This means that these strange observations were only made twice. We believe, that the data shown in Fig. 7 were obtained correctly and that perhaps during the preparation and the mounting of the samples they underwent some plastic deformation increasing the number of nucleation sites for α-ferrite formation with respect to that of all the other specimens investigated in the present work. We would like to remind the reader that we believe to have shown that nucleation must be provided for the formation of α-ferrite. Nucleation is caused by the presence of α'-martensite and dislocations, by stress, and by irradiation with high energy particles. We may state that additional nucleation is caused if the applied stress increases beyond 50 MPa (Fig. 7).

A similar qualitative observation, which has been shown in Fig. 7, is shown in Fig. 8. The amount of elongation in primary creep stages I and II decreases with increasing applied stress. In this example the data points are obtained with greater accuracy than those in the previous figure. Up to now we have not mentioned that all the length changes were obtained during the shut down of the HFR in hot cells, and we have not discussed the influence of this procedure on the measurements of the length. In the AMCR-type alloys a hexagonal martensitic ε-phase is formed below 200°C without hysteresis, which is connected with a volume change. However, with the depletion of nickel in the austenitic γ-phase during irradiation the transition temperature for the γ-ε-transformation increases accordingly so that at ambient temperature the γ-ε-transformation may not be complete, depending very much on the actual measuring temperature. Thus the scattering of the measuring data shown in Fig. 7 is rather due to the amount of the ε-phase present during the measurement of the length than to an inaccuracy in the measurements of the length.

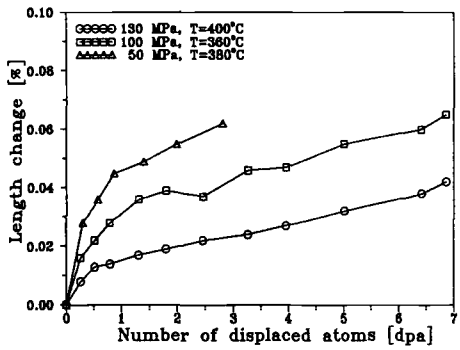

Fig. 8.
The changes in the length of three samples of AMCR 0033 are plotted versus the number of displaced atoms. The irradiation temperature and the respective applied stresses are listed in the figure. The samples were irradiated in the as-received state.

We re-plotted the data obtained for AMCR 7763 from reference [3] in Fig. 9. The specimens were solution annealed prior to irradiation. The various stresses and irradiation temperatures are indicated in the figure.

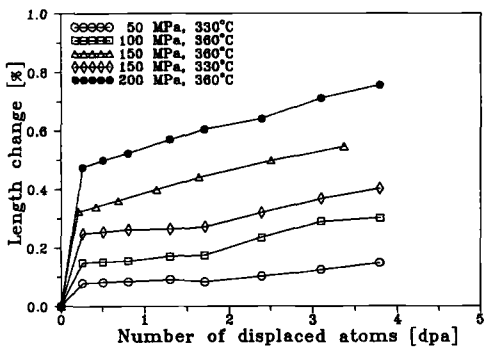

Fig. 9.
The changes in the length of samples of AMCR 7763 are plotted versus the number of displaced atoms. The irradiation temperature and the respective applied stresses are listed in the figure. The samples were solution annealed prior to irradiation.

A huge increase in length increasing with increasing applied stress is found. In primary creep stage II a further increase of the length with irradiation dose is observed, the rate of which increases with increasing applied stress. It is known that the formation of titanium carbides in steels is connected with a very large increase in volume [10]. Thus we attribute the huge length change observed to the volume change due to the formation of titanium carbide during irradiation, which was dissolved during the solution anneal prior to irradiation, hiding the volume change due to the formation of α-ferrite.

If the as-received AMCR 7763 material is annealed for one hour at 700°C then the changes in length with irradiation time are very similar to those reported for AMCR 0033 (Fig. 1). We plotted the increase in length obtained for primary creep stage I of AMCR 7763 from Fig. 9 versus the applied stress in Fig. 10.

The length change increases approximately with the square of the applied stress and we conclude that the carbides are formed in a longish shape in the direction of the applied stress, the length of which increases with increasing applied stress. This means that the length change obtained during irradiation in primary creep stage I (Fig. 10) must be mainly due to stress-oriented formation of carbides and not to the formation of carbides which causes an extension in the volume equally in all three dimensions. If this conclusion is correct, then carbides formed prior to irradiation will also be aligned to the direction of an applied stress during irradiation with high energy particles. Thus the change in volume due to formation of carbides under an applied stress cannot be calculated just from measurements of the increase in length obtained during irradiation.

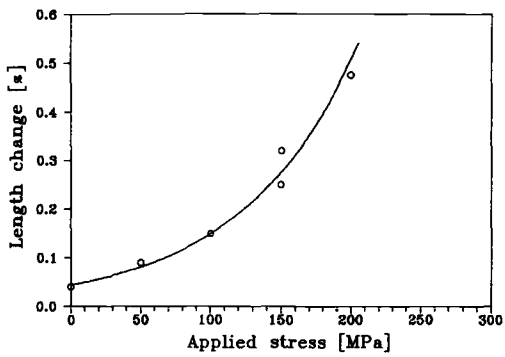

Fig. 10.
The length change of primary creep stage I of AMCR 7763 at 330-360°C from Fig. 9 in % is plotted versus the applied stress.

We concluded from the results shown e.g. in Figs. 1 to 4, that the volume of a stainless steel sample decreases, if α-ferrite is formed and that the amount of α-ferrite formed increases with decreasing irradiation temperature and with decreasing applied stress. This may mean that the α-ferrite phase could also be formed in a stress-oriented way and the volume change due to the formation of α-ferrite cannot be calculated from the decrease of the length, which is observed during irradiation. This means further that the portions of carbides and α-ferrite formed during irradiation may approximately only be obtained from experiments in which the applied stress is small while varying the irradiation temperatures (Fig. 5).

AMCR 0033 Irradiated in the Crisp Rig

It has been shown that ε-martensite, a hexagonal phase, is formed during cooling below the transition temperature without hysteresis [6]. The transition temperature of this phase decreases slightly from 200°C for AMCR 0033, which contains 17.50 weight%, with increasing content of manganese. The formation of the ε-phase is accompanied with a volume change and the questions arose, whether the length changes achieved during irradiation and measured during the shut down of the reactor at ambient temperature are not falsified with respect to the length change achieved at the irradiation temperature, and whether the ε-phase formed during cooling acts as nucleation sites for α-ferrite formation during a subsequent irradiation. The relatively large scatter, which we found on measuring the variation in length at ambient temperature with irradiation time (Fig. 7), may be explained with the finding that the γ-ε transformation, the transition temperature of which is about 200°C, is not completed at ambient temperature [6].

It was further found that the ε-phase does not act as nucleation sites for the formation of α-ferrite, perhaps because it is dissolved during heating before the component atoms of the alloys are sufficiently mobile for thermal equilibrium structures to be obtained [6]. In Fig. 11 we plotted the results of measurements of the creep elongation for three specimens versus the neutron irradiation time for an irradiation temperature of $T_{irr.}$ = 400°C.

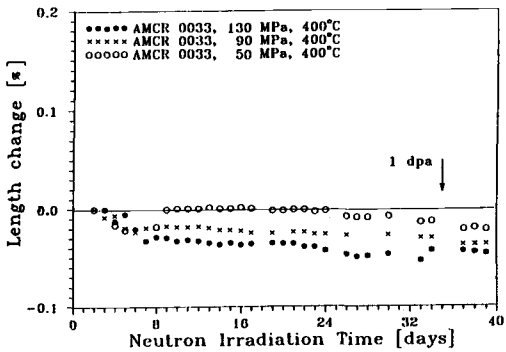

Fig. 11.
The length changes of three specimens of AMCR 0033 are plotted versus the number of displaced atoms for an irradiation temperature of $T_{irr.}$ = 400°C. The specimens were irradiated in the as-received state, and after 10% and 20% cold-worked prior to irradiation and the applied stresses were 50, 90, and 130 MPa, respectively. The variations of the length were obtained from the difference between the actual length change of the specimen and that of a dummy specimen, which was prepared like the actual specimen and irradiated without an applied stress.

It is noticed that the lengths of the specimens decrease about linearly with the number of displaced atoms and that the amount of decrease increases with increasing applied stress with respect to the changes in length of the dummy specimens. This means that the lengths of the actual specimens decreased with respect to that of the dummy specimens, which obtained the same pre-treatment as the actual specimens, respectively, and which were irradiated at the same temperature as the actual specimens, however, without an applied stress. This result is further evidence that the negative length changes observed under certain conditions (Figs. 2 to 4) are real and neither due to martensitic transformations which may occur during cooling stainless steel materials from the irradiation temperature to ambient temperature, nor to errors in the determination of the length.

However, the interpretation of the finding shown in Fig. 11 is not simple. Thus it follows that the decrease in length in primary creep stage I between the stressed and non-stressed samples is small increasing with applied stress. A similar feature according to which the change in length in primary creep stage I and the rate of the length change in primary creep stage II decreases with increasing applied stress was reported in Figs. 7 and 8. This could mean that the number of nucleation sites for α-ferrite formation increases with increasing applied stress and that the specimens must have undergone a small plastic deformation during their preparation and during mounting. The specimens used in the Crisp-rig are three times longer than those used in the Trieste-rig and for this reason the risk of an additional plastic deformation of the specimens when they are being prepared is much greater in the Crisp experiment than in the Trieste experiment.

On Secondary Irradiation Creep Rates of Stainless Steel Alloys in HFR, ORR, and EBR II

The length changes reported previously, namely for primary creep stages I and II, are attributed mainly to microstructural changes. The length changes found depend on the microstructure in the materials prior to irradiation, on the micro-structure developing during irradiation, on the irradiation temperature, on the irradiation flux, on the applied stress, and last but not least on the structures and concentrations of dislocations. This means that the term microstructure in a broader sense contains also the dislocation network present prior to irradiation and developing during irradiation. We believe that the length changes due to radiation-induced microstructural changes are for irradiation doses up to about 5 dpa larger than the length changes due to irradiation creep, and that the length changes obtained for irradiation doses larger than about 5 dpa are mainly determined by irradiation creep. We believe further that the thermal equilibrium microstructure, e. g. equilibrium phases and equilibrium dislocation structure, is approximately obtained after an irradiation dose of 5 dpa. However, for high irradiation temperatures, e.g. 500 or 600°C, the thermal equilibrium network of dislocations during irradiation is only obtained for irradiation doses as high as 45 dpa and 20 dpa, respectively (see e.g. reference [2]). Th+us the irradiation creep rates of materials, i.e. the secondary irradiation creep rates, which were obtained for annealed and cold-worked materials prior to irradiation, should be slightly different for an irradiation dose of 5 dpa.

We plotted the irradiation creep rates for 20% cold-worked AMCR 0033 and for AMCR 0033 annealed for one hour at 400°C prior to irradiation versus the reciprocal irradiation temperature in Fig. 12.

The creep rates, which follow approximately straight lines in an Arrhenius plot (Fig. 12), are slightly larger for annealed than for cold-worked materials. However, the activation energy resulting for the irradiation creep rates from the slopes of the straight lines is $Q_{irr.}$= 0.132 eV for both materials. Thus the irradiation creep rate $\dot{\varepsilon}$ is:

$$\dot{\varepsilon} = C_1 \exp.\left(-\frac{Q_{irr.}}{k\,T}\right) \qquad (1)$$

Apparently constant C_1 is slightly different for annealed and for cold-worked materials after an irradiation dose of 5 dpa, which is not surprising because the thermal dynamic equilibrium concentrations of dislocations are assumed not to be completely obtained for 5 dpa. The small activation energy of $Q_{irr.}$= 0.132 eV has been observed previously in many different laboratories and appears to be a general feature of irradiation creep [12-15].

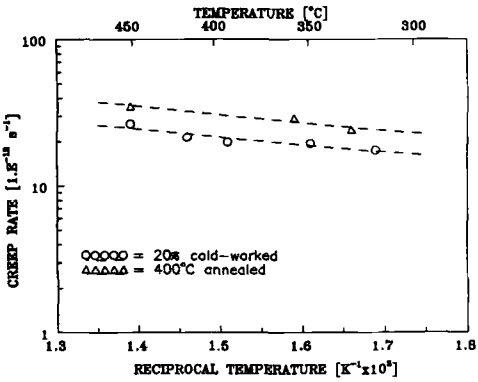

Fig. 12.
The logarithm of the creep rate of AMCR 0033 materials annealed for one hour at 400°C and 20% cold-worked prior to irradiation is plotted versus the reciprocal irradiation temperature. The radiation damage rate was $1.5 \cdot 10^{-7}$ dpa·s^{-1}. The creep rates were determined for 5 dpa.

The explanation of this small activation energy of Q_{irr}= 0.132 eV is not simple. We know that all the microstructure developing during irradiation is formed by diffusing radiation-produced interstitials and vacancies, also the dislocation network. If all the radiation-produced point defects annihilate at sinks, e.g. at precipitates, at agglomerates of point defects, and at dislocations, then the activation energy of radiation-enhanced diffusion is zero [11]. If a very small portion of the radiation-induced point defects annihilates by pair recombination then the activation energy of diffusion is very slightly larger than zero.

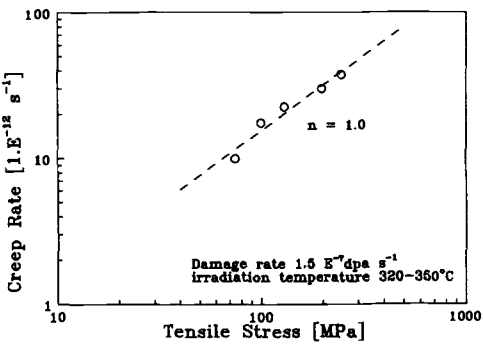

Fig. 13.
The logarithm of the creep rate of AMCR 0033 materials 20% cold-worked prior to irradiation is plotted versus the reciprocal irradiation temperature. The radiation damage rate was $1.5 \cdot 10^{-7}$ dpa·s^{-1}. The creep rates were determined for 5 dpa.

Further, if almost all the point defects annihilate at sinks then the diffusion rate increases approximately linearly with the increase of the production rate of point defects, K, i.e. with the increase of the high energy particle flux. This dependence has not been

determined in the present work, but it is known from many previous experimental results [12-15], that the irradiation creep rate is linearly increasing with increasing high energy particle flux for irradiation temperatures smaller than 450°C. Thus we believe that equation (1) can be re-written in the following way:

$$\dot{\varepsilon} = C_2 K^m \exp.\left(-\frac{Q_{irr.}}{k\,T}\right) \qquad \text{where } m = 1, \text{ for } T<723K \qquad (2)$$

where C_2 is a new constant which again is slightly different for annealed and cold-worked materials.

We plotted the irradiation creep rate versus the applied stress σ in Fig. 13. The stress exponent resulting from the curve in Fig. 13 is $n \approx 1$. Similar stress exponents have been reported in the literature for many years for irradiation temperatures lower than about 450°C [12-15]. Thus, we believe that equation (1) can be re-written in the following way:

$$\dot{\varepsilon} = C_3 \sigma^n K^m \exp.\left(-\frac{Q_{irr.}}{k\,T}\right) \qquad \text{where } n = 1 \text{ for } T<723K \qquad (3)$$

C. Wassiliew et al. [12] assumed that the activation energy $Q_{irr.} = 0.132$ eV, which they also obtained for various types of stainless steel materials for the temperature region below 550°C, would be approximately the migration activation energy of interstitials. We have shown in the past that interstitials in fcc materials migrate and annihilate in recovery stage III, which means that the migration activation energy of interstitials in stainless steel alloys is $E_{II}^{M} \approx 1.0$ eV [16]. If the migration activation energy of interstitials were as small as C. Wassiliew et al. are assuming, then the concentration of interstitials built up during irradiation at 500°C would be so small that no agglomerates of interstitials and in turn no dislocation network would be formed in contradiction to the well established experimental results.

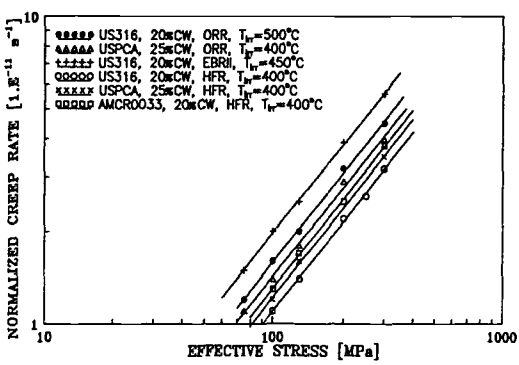

Fig. 14.
The logarithm of the normalized creep rates of AMCR 0033, US 316, US PCA and European reference steel 316L obtained at HFR, ORR and EBR II are plotted versus the applied stress for irradiation temperatures below 450°C. It was assumed that the radiation damage rates were $1.5 \cdot 10^{-7}$, $1.4 \cdot 10^{-7}$, $6.0 \cdot 10^{-7}$ dpa·s^{-1} for HFR, ORR, and EBR II, respectively. The creep rates were determined for 5 dpa.

It has also be well known for many years that the creep rate increases drastically with increasing irradiation temperature above a characteristic temperature, which is about 450°C in stainless steel alloys, regardless of whether the irradiations are performed in fast reactors or with high energy protons. The activation energies above this characteristic temperature finally achieve the activation energy of self-diffusion [12-15]. This means that the creep rates above this characteristic temperature are determined simultaneously by self-diffusion and radiation-enhanced diffusion. Consequently, the creep rates given by equation (3) are not valid for irradiation temperatures above about 450°C. Above this temperature the activation energy becomes much larger than $Q_{irr.}$= 0.132 eV and the stress exponent is also much larger than n =1.

In Fig. 14 we plotted the secondary creep rates normalized to the number of displaced atoms for AMCR 0033, US 316, US PCA, and European reference steel obtained in HFR, and also in ORR and in EBR II versus the applied stress for irradiation temperatures smaller than 500°C. All the materials were 20 % cold-worked prior to irradiation. It is seen from Fig 14 that the normalized creep rates of all types of austenitic steels investigated in the present work are very similar within the error limits and in agreement with the results obtained in ORR and EBR II. Thus we are able to evaluate approximately the constant C_3 of equation (3) from the results shown in Fig. 14 to $C_3 = 1.3 \cdot 10^{-5}$ [$dpa^{-1} \cdot MPa^{-1}$].

CONCLUSIONS

The main important radiation damage produced in solid materials by high energy particle irradiation, e.g. by high energy electrons or 14 MeV neutrons, is interstitials and vacancies. The migration and reaction of these two types of point defects lead to agglomerates of interstitials and vacancies, respectively, the transition temperature of which is $T_t \approx 340$°C in stainless steel alloys. Below this temperature agglomerates of interstitials are formed, and above this temperature agglomerates of vacancies are formed. Microstructural changes, e.g. changes in the geometrical arrangement of component atoms in an alloy, are obtained by diffusing point defects produced by irradiation with high energy particles.

The many different phases present in stainless steel alloys will be enriched in nickel through radiation-enhanced diffusion, because nickel diffuses faster than iron and chromium in stainless steel alloys. For the formation of α-ferrite, which is formed during irradiation in stainless steel alloys by radiation-enhanced diffusion, nucleation is necessary. Nucleation of this phase is obtained by irradiation with high energy particles, by deformation, or by an applied stress only.

Radiation-induced microstructures, e.g. nickel-silicon precipitates in stainless steel alloys, are obtained by irradiating below the transition temperature for the formation of agglomerates of interstitials.

All the microstructure, e.g. all phases and compounds, formed during irradiation in stainless steel alloys, is connected with volume changes. The formation of α-ferrite causes a decrease and the formation of carbides an increase in volume, and these two phases are

considered mainly responsible for the length changes measured in the present work up to irradiation doses of about 5 dpa.

The amount of α-ferrite formed during irradiation increases with decreasing irradiation temperature and with decreasing applied stress. α-ferrite is brittle and leads to fracture of the materials for irradiation temperature of e.g. 60 and 100°C. The amount of α-ferrite formation decreases with decreasing irradiation temperature.

The increase in volume due to carbide formation is especially large for titanium carbide formation. Stress-oriented formation of carbides was also observed.

The formation of microstructure during irradiation due to a geometrical re-arrangement of component atoms is approximately completed after a dose of about 5 dpa. The formation of a dynamic equilibrium dislocation network, which is also part of the microstructure evolution during irradiation, is obtained after irradiation doses of 20 dpa at about 500°C. This means that the irradiation creep rate follows equation (3). The constant C_3 varies slighlty between 5 and 20 dpa depending on the concentration of the dislocation network achieved.

The results of the present work suggest that titanium-modified and solution-annealed steels should not be used in nuclear reactors, but instead aged or cold-worked stainless steel alloys. It is further suggested, that the service temperature of a nuclear reactor should be well above 100°C if stainless steel alloys are considered. A service temperature of about 340°C would be a good choice, because hardly any radiation-induced structures are formed during irradiation [16]. It is assumed that the amount of α-ferrite formed during irradiation in 316- and AMCR-type alloys decreases, if more nickel or more manganese, respectively, is added to these alloys.

ACKNOWLEDGEMENT

We would like to thank the staff of the former Reactor Division of the Joint Research Center of Petten, The Netherlands, for their kind collaboration during the last 18 years. We especially thank Mr. P. von der Hardt, who always supported this research and Mr. R. Lölgen, who was responsible for the construction of the very fancy irradiation creep facilities Trieste and Crisp.

REFERENCES

[1] International Symposia on Effects of Radiation on the Microstructure of Materials, Philadelphia, USA, ASTM STP 1125, STP 1046, STP 955, and etc..

[2] F. A. Garner, Irradiation Performance of Cladding and Structural Steels in Liquid Metal Reactors, Materials Science and Technology, R. W. Cahn, P. Haasen, and E. J. Kramer, Eds., Nuclear Materials, B. R. T. Frost, Ed., Part I, Vol. 10A, 1994, pp. 419-543.

[3] W. Schüle and H. Hausen, Sixth International Conference on Fusion Reactor Materials (ICFRM-6), Stresa, Lago Maggiore, Italy, September 27-October 1, 1993, D. G. Rickerby, H. Stamm, K. Ehrlich, and M. Victoria, Eds., Journal of Nuclear Materials, Vols. 212-215, 1994, pp. 388-392.

[4] M. L. Grossbeck, L. T. Gibson, and S. Jitsukawa, 7th International Conference on Fusion Reactor Materials, (ICFRM-7), V. M. Chernov, W. M. Gauster, D. S. Gelles, A. B. Hull, R. L. Klueh, and H. Stamm, Eds., Obninsk, Kaluga Region, Russia, September 25-29, 1995, Journal of Nuclear Materials, Vols. 233-237, 1996, pp. 148-151.

[5] H. Hausen and W. Schüle, "Neutron Irradiation Creep at 100°C on 316L, on AMCR, and on Welded 316L Stainless Steel Alloys", This conference.

[6] W. Schüle and E. Lang, 15th International Symposium on Effects of Radiation on Materials, R. E. Stoller, A. S. Kumar, and D. S. Gelles, Eds., American Society for Testing and Materials, Philadelphia, ASTM STP 1125, 1992, pp. 945-957.

[7] A. Tas and G. J. A. Teunissen, "Users Report of HIP-TEDDI", Report EUR 5700 EN (1978).

[8] F. A. Garner and H. R. Brager, 13th International Symposium on Radiation-Induced Changes in Microstructure, F. A. Garner, N. H. Packan, and A. S. Kumar, Eds., Seattle, WA, USA, 23-25 June, 1986, American Society for Testing and Matertials, ASTM STP 955, 1987, pp. 195-206.

[9] H. Hausen, W. Schüle, and M. R. Cundy, Proceedings of the 15th International Symposium on Fusion Technology, 15th SOFT, 9-13 September 1988, Utrecht, The Netherlands, A. M. Van Ingen, A. Nijsen-Vis, and H. T. Klippel, Eds., Fusion Technology, Vol. 2, 1988, pp. 905-909.

[10] P. J. Maziasz, Proceedings of a Symposium on Phase Stability during Irradiation, Fall Meeting of The Metallurgical Society of AIME, Pittsburgh, Pennsylvania, USA, October 5-9, 1980, J. R. Holland, L. K. Mansur, and D. I. Potter, Eds., The Metallurgical Society of AIME, 1981, p. 477- 492.

[11] W. Schüle, E. Lang, D. Donner, and H. Penkuhn, Radiation Effects, Volume 2, 1970, pp. 151-163.

[12] C. Wassiliew, K. Ehrlich, and H.-J. Bergmann, 13th International Symposium on the Influence of Radiation on Material Properties, F. A. Garner, C. H. Henager, Jr., and N. Igata, Eds., Seattle, WA, USA, 23-25 June, 1986, American Society for Testing and Materials, ASTM STP 956, 1987, pp. 30-53.

[13] E. R. Gilbert, and J. F. Bates, Proceedings of an International Conference on Measurements of Irradiation-Enhanced Creep in Nuclear Materials, M. R. Cundy, P. von der Hardt, and R. H. Loelgen, Eds., Petten, The Netherlands, May 4-6., 1976, North Holland Publishing Company, Amsterdam, 1977, pp. 204-209.

[14] E. R. Gilbert, J. L. Straalsund, and G. L. Wire, Proceedings of an International Conference on Measurements of Irradiation-Enhanced Creep in Nuclear Materials, M. R. Cundy, P. von der Hardt, and R. H. Loelgen, Eds., Petten, The Netherlands, May 4-6, 1976, North Holland Publishing Company, Amsterdam, 1977, pp. 266-278.

[15] J. A. Hudson, R. S. Nelson, and R. J. McElroy, Proceedings of an International Conference on Measurements of Irradiation-Enhanced Creep in Nuclear Materials, M. R. Cundy, P. von der Hardt, and R. H. Loelgen, Eds., Petten, The Netherlands, May 4-6, 1976, North Holland Publishing Company, Amsterdam, 1977, pp. 279-294.

[16] W. Schüle, Zeitschrift für Metallkunde, Vol. 85, 1994, pp. 78-91.